

## Design of combined non-tracking concentrated optical system

Ru Zhanqiang, Song Helun, Wu Fei, Song Shengxing, Zhu Yu, Yin Zhizhen, Zhang Yaohui

(System Integration & IC Design Division, Suzhou Institute of Nano-tech and Nano-bionics,  
Chinese Academy of Sciences, Suzhou 215123, China)

**Abstract:** A combined non-tracking concentrated optical (CNTCO) system composed of line Fresnel lens (LFL), reflection-type secondary optical element(R-SOE) and total internal reflection prism (TIRP) was proposed due to the high failure rate and high cost of the automatic solar tracking system. Moreover, the principle and design method of each component were discussed. The structure of the system was optimized and simulated in optical design software Zemax. The results show that the average concentration efficiency of the system reaches up to 24.1%, an 18.7% increasement compared with a combined system consisted of LFL and R-SOE (FRS), on the condition that the pitch angle is up to 16°. The non-tracking concentrated photovoltaic module based on CNTCO system was integrated and preliminarily tested. The test results indicate that the photoelectric transformation efficiency of the module could be optimized up to 19.6% on non-tracking condition, even still up to 5.9% after 4 hours.

**Key words:** optical design; non-tracking concentrated optical system; combinatorial optimization; line Fresnel lens; secondary optical element

**CLC number:** O435 **Document code:** A **DOI:** 10.3788/IRLA201948.0318002

## 组合式免跟踪聚光光学系统设计

茹占强, 宋贺伦, 吴 菲, 宋盛星, 朱 煜, 殷志珍, 张耀辉

(中国科学院苏州纳米技术与纳米仿生研究所 系统集成与 IC 设计研究部, 江苏 苏州 215123)

**摘 要:** 针对当前聚光光伏系统中自动跟踪系统故障率高及跟踪成本大等问题, 提出了一种由线聚焦菲涅耳透镜、反射式二次聚光器和全反射棱锥组成的组合式免跟踪聚光光学系统, 论述了各组成元件的工作原理与设计方法。在光学设计软件 Zemax 里对该系统进行结构优化与仿真分析, 结果表明, 在俯仰角最大为 16° 时, 该系统的平均聚光效率为 24.1%, 与 FRS 系统相比提高了 18.7%。集成了基于组合式免跟踪聚光光学系统的免跟踪聚光光伏模组, 初步测试结果表明, 该模组在非跟踪状态下光电转换效率最高达到 19.6%, 4 h 后光电转换效率仍能达到 5.9%。

**关键词:** 光学设计; 免跟踪聚光光学系统; 组合优化; 线聚焦菲涅耳透镜; 二次聚光器

收稿日期: 2018-10-10; 修订日期: 2018-11-28

基金项目: 国家重点研发计划(2016YFE0129400); 国家自然科学基金面上项目(51377159); “十三五”国家密码发展基金(MMJJ20180112); 中国科学院青年创新促进会人才资助计划(2016290)

作者简介: 茹占强(1982-), 男, 助理研究员, 硕士, 主要从事聚光光伏技术方面的研究。Email: zqru2008@sinano.ac.cn

通讯作者: 宋贺伦(1980-), 男, 研究员, 博士, 主要从事聚光光伏技术、半导体器件集成等方面的研究。Email: hlsong2008@sinano.ac.cn

## 0 Introduction

In photovoltaic field, the concentrated optics is introduced into photovoltaic system for reducing cost of photovoltaic power generation<sup>[1-2]</sup>. This photovoltaic system containing concentrated optics is called concentrated photovoltaic (CPV) system, it can reduce the area of expensive solar cell<sup>[3-5]</sup>, whereas a two-dimensional automatic solar tracking system has to be introduced. The automatic solar tracking system has many disadvantages, for example, high failure rate, poor maintainability, high cost and noise etc., especially in extreme environments, although it is not difficult to achieve automatic tracking through mature automatic control technology<sup>[6-7]</sup>. Therefore, it still remains a problem in the practical application of photovoltaic system. At the same time, the introduction of a tracking system will significantly increase the cost of photovoltaic power generation.

Therefore, a CNTCO system is proposed, which has high concentration efficiency still on the condition of large incidence angle. So the automatic solar tracking system is not necessary in photovoltaic system.

The CNTCO system is suitable for low concentration photovoltaic system, which is helpful for simplifying the configuration and complexity of photovoltaic system, and reducing cost of the photovoltaic power generation.

## 1 Basics of design

The premise of designing a CNTCO system is based on the relative position of the sun and the earth. The rotation of the earth around its polaxis and the sun from west to east at a speed of  $15^\circ/h$  causes the direction and intensity of sunlight to vary continuously<sup>[8-9]</sup>. Taking ground coordinates as a reference system, the pitch angle and azimuth

angle of the sun will be changed every day, as shown in Fig.1.

Take Suzhou as an example, which is located at  $31.3^\circ N$  and  $120.6^\circ E$ , the maximum variation range of the pitch angle is  $\delta = \pm 16^\circ (50^\circ - 82^\circ)$  in the summer solstice according to the calculation formula of "The criterion of surface meteorological observation". At the same time, the effective variation range of the azimuth angle is  $\theta = \pm 60^\circ$ , because the solar cell can't work normally on the condition that the light intensity is weak in the morning and afternoon.

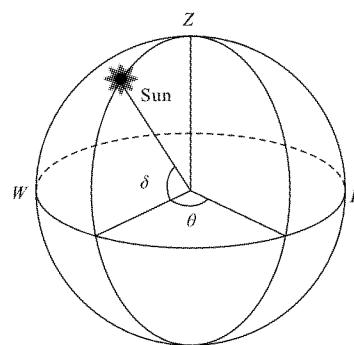


Fig.1 Position of the sun in the ground coordinate system

Therefore, the effective concentrated angle range of CNTCO system should be larger than the variation range of the pitch angle and azimuth angle of the sun.

## 2 Design of CNTCO system

According to the variation range of  $\delta = \pm 16^\circ$  and  $\theta = \pm 60^\circ$ , a CNTCO system is proposed in this paper, as shown in Fig.2 and Fig.3, which is

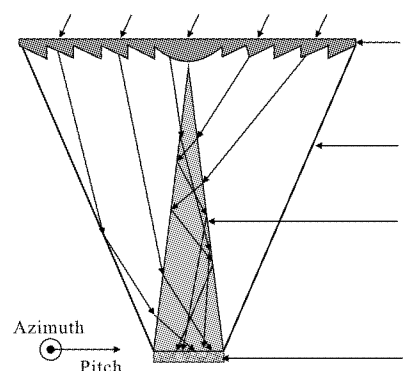


Fig.2 Schematic of CNTCO working system

composed of line Fresnel lens 1, reflection-type secondary optical element 2 and total internal reflection prism 3, and where 4 represents solar cell.

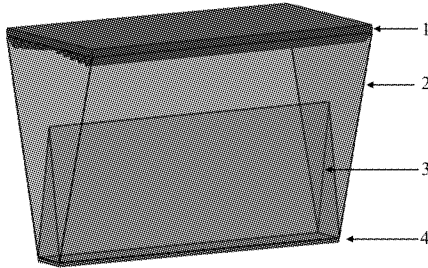


Fig.3 Structure diagram of CNTCO system

### 2.1 Line Fresnel lens

The line Fresnel lens (LFL) is engraved with a series of zigzag stripes that are symmetrical along the axis plane. Light incident on the LFL is concentrated on a focal line by zigzag stripes, as shown in Fig.4.

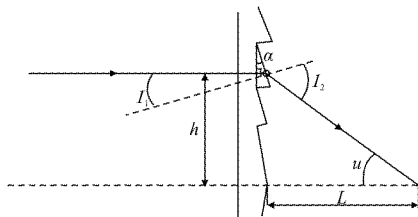


Fig.4 Optical path diagram of LFL

Where  $h$  represents the distance from the incident light to the axis plane,  $L$  stands for the focal length of LFL,  $u$  is the angle of concentration, and  $\alpha$  is the inclination of zigzag stripe. According to the law of Fresnel, the formula is:

$$u = \arctan\left(\frac{h}{L}\right) \quad (1)$$

$$\alpha = \arctan\left(\frac{\sin u}{n - \cos u}\right) \quad (2)$$

As long as the material and focal length are determined, the inclination of each zigzag strip can be calculated according to Eq.(1) and Eq.(2), so the LFL is modeled and simulated in the non-sequential mode of optical design software Zemax according to the inclination of each zigzag strip<sup>[10-12]</sup>, as

shown in Fig.5. The concentration efficiencies of the LFL at different incident angles are listed in Tab.1.

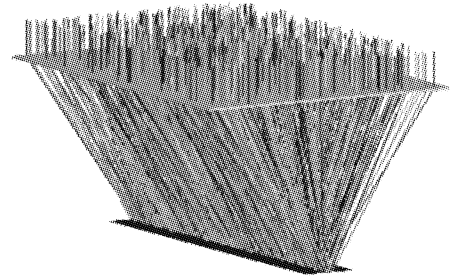


Fig.5 Modeling and simulation of LFL in Zemax

Tab.1 Concentration efficiencies of the LFL

| Pitch angle/(°) | Concentration efficiency | Azimuth angle/(°) | Concentration efficiency |
|-----------------|--------------------------|-------------------|--------------------------|
| 0               | 90.9%                    | 0                 | 90.9%                    |
| 4               | 66.0%                    | 15                | 76.1%                    |
| 8               | 8.2%                     | 30                | 40.8%                    |
| 12              | 0.6%                     | 45                | 11.8%                    |
| 16              | 2.8%                     | 60                | 1.4%                     |

### 2.2 Reflection-type secondary optical element

According to Tab.1, the acceptance angle of LFL is very small in the pitch direction. Meanwhile, based on the principle, the LFL can't concentrate light in the azimuth direction, thus the edge light rays will deflect out of the solar cell provided the azimuth angle is not zero. Therefore, a reflection-type secondary optical element (R-SOE) is proposed, which has an inverted trapezoidal trough structure with open ends, as displayed in Fig.3. Its four inner surfaces are coated with a highly reflective aluminum film, and two end surfaces reflect the edge rays to the solar cell again, and two side surfaces concentrated the defocused rays to the focal line again. By changing the degrees of the side surface incline, it can concentrate rays of different defocusing amount<sup>[13-14]</sup>, so we can find an optimized inclining degree which can maximize the system's concentration efficiency. The LFL and the optimized R-SOE make up a concentrated optical

system (FRS), the concentration efficiencies of the FRS system at different incident angles are listed in Tab.2.

**Tab.2 Concentration efficiencies of the FRS system**

| Pitch angle/(°) | Concentration efficiency | Azimuth angle/(°) | Concentration efficiency |
|-----------------|--------------------------|-------------------|--------------------------|
| 0               | 87.3%                    | 0                 | 87.3%                    |
| 4               | 72.1%                    | 15                | 85.5%                    |
| 8               | 45.1%                    | 30                | 76.3%                    |
| 12              | 26.5%                    | 45                | 45.2%                    |
| 16              | 4.3%                     | 60                | 20.8%                    |

**2.3 Total internal reflection prism**

The R-SOE can increase the concentration efficiency under the oblique incidence condition, but when the angle reaches maximum, the increments will decrease drastically, according to the comparison between Tab.1 and Tab.2.

Therefore, a total internal reflection prism (TIRP) is introduced. The structure and principle of TIRP are depicted in Fig.3 and Fig.6, where C represents the total internal reflection critical angle. When the total internal reflection condition is satisfied, rays can propagate without energy loss in TIRP, and the solar cell can obtain more light energy, otherwise rays will be deflected downward. According to the law of Fresnel and trigonometric formulas, the formula of the TIRP can be expressed as:

$$n^2 \sin\beta = \sqrt{n^2 - \sin^2 R_1} - \sin R_1 \sqrt{n^2 - 1} \quad (3)$$

By changing the value of  $\beta$ , the solar cell can obtain different light energies according to Eq.(3). Consequently, taking concentration efficiency as the target, and taking  $\beta$  as a variate to optimize the structure of TIRP in the non-sequential mode of Zemax. The LFL, optimized R-SOE and optimized TIRP make up the combined non-tracking concentrated optical (CNTCO) system. The concentration efficiencies of the CNTCO system at different incident angles are listed in

Tab.3.

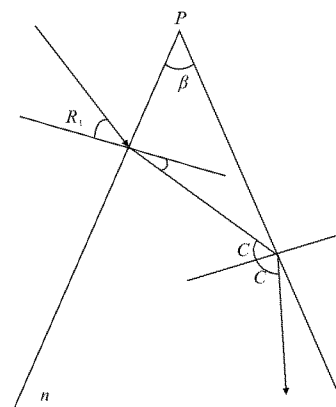


Fig.6 Schematic of TIRP

**Tab.3 Concentration efficiencies of the CNTCO system**

| Pitch angle/(°) | Concentration efficiency | Azimuth angle/(°) | Concentration efficiency |
|-----------------|--------------------------|-------------------|--------------------------|
| 0               | 81.2%                    | 0                 | 81.2%                    |
| 4               | 74.3%                    | 15                | 79.3%                    |
| 8               | 47.2%                    | 30                | 70.4%                    |
| 12              | 34.1%                    | 45                | 52.7%                    |
| 16              | 24.9%                    | 60                | 28.5%                    |

**3 Results discussion**

In this section, the performance of the proposed CNTCO system is examined. The optimized CNTCO system parameters configured in the simulation and experiment are listed in Tab.4.

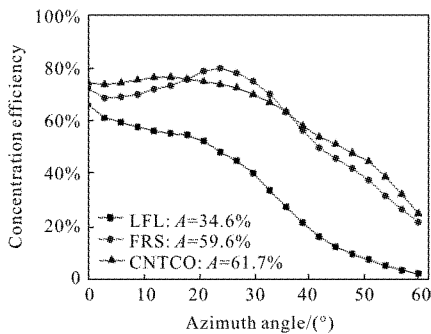
**Tab.4 CNTCO system parameters**

| CNTCO system parameters              | Values |
|--------------------------------------|--------|
| Pitch aperture of LFL/mm             | 350    |
| Azimuth aperture of LFL/mm           | 500    |
| Focal length of LFL/mm               | 250    |
| Top aperture of R-SOE/mm             | 350    |
| Bottom aperture of R-SOE/mm          | 70     |
| Incline of side surface of R-SOE/(°) | 47     |
| Bottom aperture of TIRP/mm           | 70     |
| $\beta$ of TIRP/(°)                  | 38.6   |

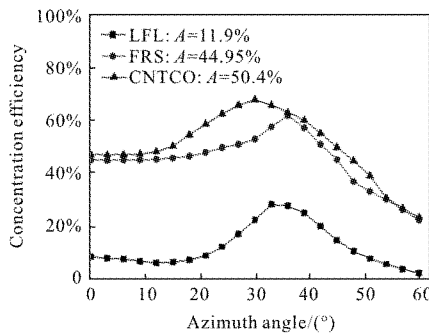
As described above, the concentration efficiencies of LFL, FRS system and CNTCO

system have been contrasted in Tab.1, Tab.2 and Tab.3. However, the efficiency comparison of a single angle is little significance in practical engineering applications. It can generate more power only on the condition that average concentration efficiency is high. Consequently, LFL, FRS and CNTCO are simulated in the non-sequential mode of Zemax software, and average concentration efficiency is displayed in Fig.7, where "A" represents average concentration efficiency.

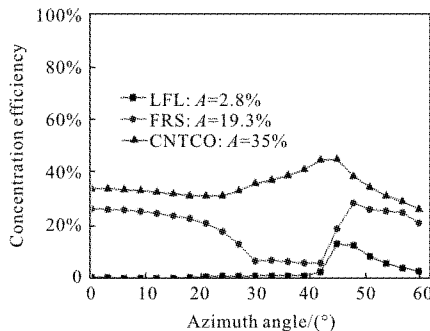
The simulation results indicate that the average concentration efficiency of CNTCO system is up to 61.7%, 50.4%, 35% and 24.1% respectively when the pitch angle is 4°, 8°, 12° and 16°.



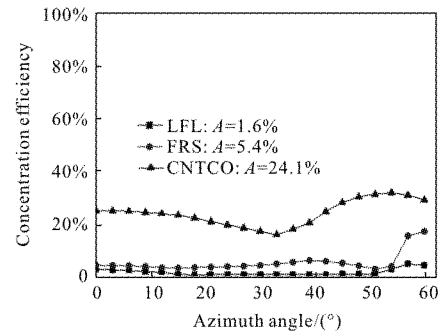
(a) Pitch angle 4°



(b) Pitch angle 8°



(c) Pitch angle 12°



(d) Pitch angle 16°

Fig.7 Concentration efficiencies comparison with different pitch angle

Compared with the LFL the efficiency increases by 27.1%, 38.5%, 32.2% and 22.5% respectively, and compared with FRS system the efficiency increases by 2.1%, 5.5%, 15.7% and 18.7%.

In addition, a tracking concentrated optical (TCO) system composed of point Fresnel lens (PFL) and secondary optical element (SOE) is simulated and analyzed, as shown in Fig.8 and Fig.9. The parameters of TCO system are listed in Tab.5.

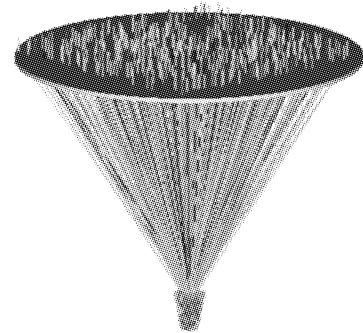


Fig.8 Modeling and simulation of TCO system in Zemax

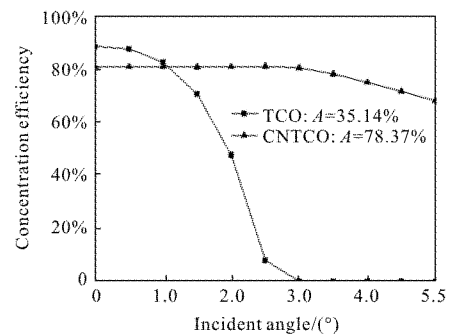


Fig.9 Concentration efficiencies comparison with different incident angles

Tab.5 TCO system parameters

| TCO system parameters              | Values |
|------------------------------------|--------|
| Aperture of PFL/mm                 | 350    |
| Focal length of PFL/mm             | 250    |
| Top aperture of SOE/mm             | 22     |
| Bottom aperture of SOE/mm          | 10     |
| Incline of side surface of SOE/(°) | 78.7   |

The results indicate that the concentration efficiency of CNTCO system is still up to about 70% when incident angle is  $5^\circ$ , in contrast, the concentration efficiency of TCO system drops to 0 when incident angle is greater than  $3^\circ$ . Consequently the TCO system has to introduce a two-dimensional automatic solar tracking system.

Meanwhile, as shown in Fig.10, a sample of the CNTCO system is realized. Based on this, the non-tracking CPV module is integrated, as shown in Fig.11. It is difficult to measure the angle of incidence accurately, consequently the photoelectric transformation efficiency of the non-tracking CPV module is tested at different time, which is depicted in Fig.12.

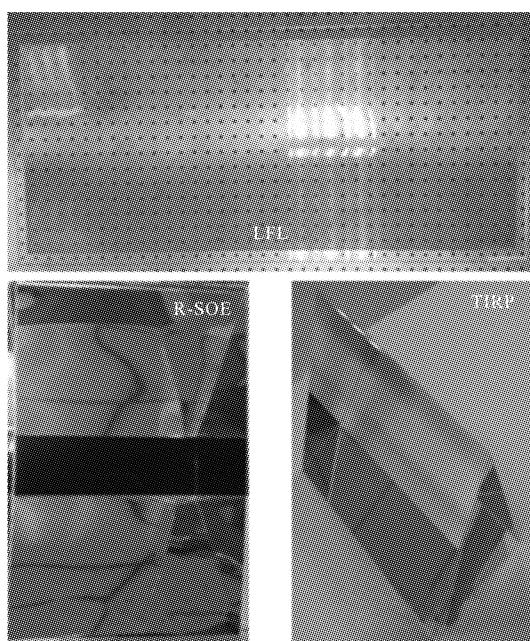
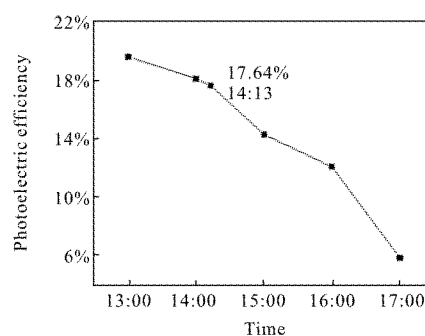


Fig.10 Sample of CNTCO system



Fig.11 Test setup of non-tracking CPV module

Fig.12  $I$ - $V$  characteristic of the non-tracking CPV module

Preliminary test result shows that the photoelectric transformation efficiency of the non-tracking CPV module reaches a maximum of 19.6% at 1 pm and decreases to 17.64% at 14:13, then to 5.9% at 5 pm. On the contrary, the photoelectric transformation efficiency of ordinary HCPV module without tracking system decreased from maximum to 0 only in 15 min<sup>[15]</sup>. Hence, the CNTCO system is robust in practical engineering applications.

## 4 Conclusions

In conclusions, we have proposed and demonstrated a combined non-tracking concentrated optical system. The system always maintains high concentration efficiency during its working time without automatic solar tracking system. Meanwhile, the CNTCO system ensures that non-tracking concentrated photovoltaic module can continuously generate electricity within 8 hours on non-tracking condition.

**References:**

- [1] Kim B, Kim J K, Park C K, et al. Design and fabrication of concentrated photovoltaic optics with high numerical aperture using a curved catadioptric optical system [J]. *Journal of Mechanical Science & Technology*, 2016, 30(3): 1315–1322.
- [2] Ghosh A, Nirala A K, Yadav H L. Wavelength selective holographic concentrator: Application to concentrated photovoltaics [J]. *Optik – International Journal for Light and Electron Optics*, 2015, 126(23): 4313–4318.
- [3] Burhan M, Chua K J E, Ng K C. Simulation and development of a multi-leg homogeniser concentrating assembly for concentrated photovoltaic (CPV) system with electrical rating analysis[J]. *Energy Conversion & Management*, 2016, 116: 58–71.
- [4] Wang Xiao, Cao Miao, An Zhiyong, et al. Design and research of total –internal –reflection solar energy concentrating module [J]. *Infrared and Laser Engineering*, 2016, 45(10): 1020001. (in Chinese)
- [5] Wattana Ratismith, Yann Favre, Maxime Canaff, et al. A non –tracking concentrating collector for solar thermal applications[J]. *Applied Energy*, 2017, 200: 39–46.
- [6] Baig H, Sellami N, Mallick T K. Trapping light escaping from the edges of the optical element in a concentrating photovoltaic system [J]. *Energy Convers Manage*, 2015, 90: 238–246.
- [7] Tharamuttam J K, Ng A K. Design and development of an automatic solar tracker [J]. *Energy Procedia*, 2017, 143: 629–634.
- [8] Canada J, Utrillas M P, Martinez –Lozano J A, et al. Design of a sun tracker for the automatic measurement of spectral irradiance and construction of an irradiance database in the 330–1100 nm range [J]. *Renewable Energy*, 2007, 32(12): 2053–2068.
- [9] Chen Y T, Ho T H. Design method of non –imaging secondary (NIS) for CPV usage[J]. *Solar Energy*, 2013, 93: 32–42.
- [10] Wang Nianju, Cai Huaiyu, Huang Zhanhua. The method of non-tracking sunlight importing lighting systems [J]. *Acta Energetica Solaris Sinica*, 2017, 38(5): 1206–1210. (in Chinese)
- [11] Li Wang, Xu Xiping, Song Helun, et al. Design and analysis of the line focus Fresnel concentrator based on the diffused focal points method[J]. *Infrared and Laser Engineering*, 2010, 39(4): 721–726. (in Chinese)
- [12] Zhang Mingjun, Gao Wenyong, Niu Quanyun, et al. Characteristics analysis and simulation of Fresnel concentrator in concentrated photovoltaic system [J]. *Infrared and Laser Engineering*, 2015, 44 (8): 2411–2416. (in Chinese)
- [13] Yang Guanghui, Liu Youqiang, Wang Yumin, et al. Design and research of secondary microprism in dense matrix type concentrating photovoltaic module [J]. *Infrared and Laser Engineering*, 2015, 44(12): 3645–3649. (in Chinese)
- [14] Toyoda H, Mukohzaka N, Mizuno S, et al. Column parallel vision system (CPV) for high-speed 2D image analysis [C]//Proceedings of SPIE –The International Society for Optical Engineering, 2001, 4416: 256–259.
- [15] Renno C, Landi G, Petito F, et al. Influence of a degraded triple-junction solar cell on the CPV system performances [J]. *Energy Conversion & Management*, 2018, 160: 326–340.